

Received March 1, 2020, accepted March 8, 2020, date of publication March 13, 2020, date of current version March 24, 2020.

Digital Object Identifier 10.1109/ACCESS.2020.2980544

# Multi-Agent Framework for Service Restoration in Distribution Systems With Distributed Generators and Static/Mobile Energy Storage Systems

PANGGAH PRABAWA, (Student Member, IEEE), AND DAE-HYUN CHOI<sup>ID</sup>, (Member, IEEE)

School of Electrical and Electronics Engineering, Chung-Ang University, Seoul 156-756, South Korea

Corresponding author: Dae-Hyun Choi (dhchoi@cau.ac.kr)

This work was supported in part by the National Research Foundation of Korea (NRF) through the Korea Government (MSIP) under Grant 2018R1C1B6000965, and in part by the Chung-Ang University Research Grants in 2019.

**ABSTRACT** This paper presents a multi-agent system (MAS)-based approach for service restoration in a distribution system with distributed generators (DGs), static energy storage systems (SESSs), and mobile energy storage systems (MESSs). In comparison with existing MAS-based service restoration approaches in a two-layer cyber-physical architecture, excluding the dispatch of MESSs, we propose a three-layer framework that consists of cyber, physical, and transportation layers corresponding to the communication scheme for the MAS, electric distribution system, and transportation network for MESSs, respectively. In the proposed MAS framework, agents communicate and cooperate with each other for service restoration without violating system operation constraints by conducting the following actions: i) Kruskal-algorithm-based island reconfiguration (switch agent), ii) generation of switching sequence and dispatches of DGs and SESSs (DG and static battery agents) under monitored loading condition (load agent), and iii) dispatch of MESSs based on optimal road routing using the Dijkstra algorithm (mobile battery agent). Case studies were carried out in an IEEE 33-bus distribution system, and the results validated the performance of the proposed approach in terms of number of restored loads and restoration time steps, voltage level, and state of charge of the SESSs and MESSs with different numbers of fault lines and SESSs/MESS, and different extents of damaged roads.

**INDEX TERMS** Service restoration, multi-agent system, mobile energy storage system, distributed generator, restoration sequence, active distribution network.

## NOMENCLATURE

The main notations used throughout this paper are summarized here. Other undefined symbols are explained within the text.

### A. SETS

$\mathcal{L}$	Set of loads in distribution network.
$\mathcal{T}$	Set of restoration scheduling horizon.
$\mathcal{G}^{\text{DG}}$	Set of DGs.
$\mathcal{G}^{\text{ESS}}$	Set of ESSs.
$\mathcal{G}^{\text{MESS}}$	Set of mobile ESSs.

The associate editor coordinating the review of this manuscript and approving it for publication was Weiguo Xia<sup>ID</sup>.

### B. VARIABLES

$I_{t,ij}$	Current magnitude from node $i$ to $j$ at time step $t$ .
$V_{t,i}$	Voltage magnitude for node $i$ at time step $t$ .
$P_{t,l}$	Real power consumption of load $l$ at time step $t$ .
$P(Q)_{t,g}$	Real(reactive) power generation output of DG $g$ at time step $t$ .
$P_{t,g}^{\text{C(D)}}$	Charging(discharging) real power of ESS $g \in \mathcal{G}^{\text{ESS}}$ and mobile ESS $g \in \mathcal{G}^{\text{MESS}}$ at time step $t$ .
$P(Q)_{t,ij}$	Real(reactive) power from node $i$ to $j$ at time step $t$ .
$\text{SOC}_{t,g}$	State of charge of ESS $g$ at time step $t$ .
$b_{t,g}^{\text{DG}}$	Binary variable for specifying real power generation status of DG $g$ at time step $t$ .

$b_{t,g}^{\text{ESS}}$	Binary variable for specifying charging and discharging status of ESS $g$ at time step $t$ .
$b_{t,ij}^{\text{BR}}$	Binary variable for specifying real power flow status from node $i$ to $j$ at time step $t$ .
$b_{t,l}^{\text{L}}$	Binary variable for specifying load consumption status at node $l$ at time step $t$ .

### C. PARAMETERS

$R_{ij}$	Resistance of the line from node $i$ to $j$ .
$X_{ij}$	Reactance of the line from node $i$ to $j$ .
$R_g$	Ramping rate of the real power output for DG $g$ .
$\omega_l$	Load priority for load $l$ .
$\eta_g^{\text{C(D)}}$	Charging(discharging) efficiency of ESS $g$ .
$Q_g^{\text{cap}}$	Energy capacity of ESS $g$ .
$V^{\text{min(max)}}$	Minimum(maximum) limit of the allowed voltage range for any node.
$P_g^{\text{min(max)}}$	Minimum(maximum) real power capacity of DG $g$ .
$Q_g^{\text{min(max)}}$	Minimum(maximum) reactive power capacity of DG $g$ .
$P_g^{\text{C,min(max)}}$	Minimum(maximum) charging real power capacity of ESS $g$ .
$P_g^{\text{D,min(max)}}$	Minimum(maximum) discharging real power capacity of ESS $g$ .
$P_{ij}^{\text{min(max)}}$	Minimum(maximum) real power flow capacity of line from node $i$ to $j$ .
$Q_{ij}^{\text{min(max)}}$	Minimum(maximum) reactive power flow capacity of line from node $i$ to $j$ .

### ABBREVIATIONS

The main abbreviations used throughout this paper are summarized here.

MAS	Multi-Agent System.
DSSR	Distribution System Service Restoration.
DER	Distributed Energy Resource.
DG	Distributed Generator.
PV	Photovoltaic.
SESS	Static Energy Storage System.
MESS	Mobile Energy Storage System.
SOC	State of Charge.
LA	Load Agent.
SA	Switch Agent.
HSA	Head Switch Agent.
DA	DG Agent.
BSDA	Black Start DA.
NBSDA	Non-Black Start DA.

### I. INTRODUCTION

For reliable and resilient operation of electric distribution systems under extreme weather conditions and potential cyber attacks, power systems have attracted much attention from both academia and industry in the context of developing self-healing smart distribution systems [1]. Self-healing

functions are typically used by system operators from a centralized distribution system control center with the aim of rapidly identifying and isolating faulty areas, and efficiently restoring the customer service. To this end, maximum load is provided to the faulty areas through network reconfiguration using remotely controllable switches (e.g., sectionalizing switches and tie switches).

Recently, electric distribution systems are being integrated with emerging smart grid technologies, including distributed energy resources (DERs) (e.g., solar photovoltaic (PV), static energy storage systems (SESSs), and mobile energy storage systems (MESSs)) and demand side management. Thus, service restoration of distribution systems through self-healing operation can be more efficiently conducted through the coordination of dispatchable DERs, controllable switches, and load shedding and shifting [2]. However, a centralized service restoration approach could be vulnerable to a single point of failure and have a significantly increasing computational complexity due to the control of a large number of heterogeneous DERs and switches along with various demand response programs. These challenges require further distributed service restoration through operations of smart distribution systems.

The procedure of a self-healing distribution system mainly consists of (1) fault identification and isolation and (2) service restoration. In the first step, measurements from protective relays and fault indicators are employed to identify faulty locations. The faulty areas are isolated by opening the adequate switches along the distribution feeder. In the second step, DERs locally support the load demand in the faulty areas, and switches automatically connect the faulty areas to non-faulty areas, thereby achieving service restoration. In this study, we assumed that fault identification and isolation operate well. Under this assumption, we addressed the aforementioned challenges for centralized service restoration. We propose a distributed multi-agent service restoration for active distribution systems with distributed generators (DGs), SESSs, and MESSs. A more detailed review of the literature related to distribution system service restoration (DSSR) allows categorization into the following three parts:

- 1) Centralized approach: To restore unserved loads quickly and efficiently, service restoration approaches were traditionally designed for centralized operation, that is, a central entity coordinates the operations of controllable switches and DERs using overall system information in an optimization framework. Service restoration algorithms were formulated in terms of a mixed-integer nonlinear programming (MINLP) problem based on the bus injection formulation [3], relaxed mixed-integer semidefinite programming (MISDP) [4] in unbalanced three-phase distribution systems, and relaxed mixed integer second-order cone programming (MISOCP) [5], [6] in balanced three-phase distribution systems. To address the increasing computational complexity of the MINLP problem, mixed-integer linear programming (MILP) was used for service restoration.

Some examples are a two-stage service restoration strategy consisting of MILP and NLP models [7], multi-time step service restoration in balanced three-phase distribution systems under cold load pickup conditions [8] and unbalanced three-phase distribution systems [9], critical load restoration using a look-ahead optimization formulation with DGs in a secondary distribution system [10], and the analysis of the stability of microgrids in terms of frequency deviation [11]. To consider the uncertainty in the load and output of DGs, robust optimization-based service restoration algorithms were developed on the basis of the information gap decision theory [12] and on a two-stage model using the column-and-constraint generation method [13].

- 2) Hierarchical distributed approach: Hierarchical distributed models and methods were developed in a multi-agent system (MAS) where all local agents communicated and cooperated with each other to complete the service restoration process in a hierarchical manner. In [14], a MAS-based approach for service restoration was initially developed in a two-level hierarchical architecture where a bus agent at the lower level communicated only with the neighboring bus agents to restore the local load, while a feeder agent at the upper level facilitated the negotiation process of all load agents globally. A two-layer framework was also presented in [15], [16]. It consisted of a zone (or region) agent and a feeder agent corresponding to the first and second layers, respectively. In this scheme, the zone agent monitors its own zone status, communicates with the corresponding feeder agent, and conducts the restoration action. The feeder agent manages the actions of the zone agents by communicating with its neighboring feeder agents. A hybrid centralized–decentralized framework integrated with DGs was presented in [17]. In this framework, load agents and feeder agents communicated and coordinated their actions for the desired service restoration. In [18], a three-layer service restoration framework was presented, which consisted of a data layer for monitoring and collecting data, an agent layer for scheduling the service restoration, and an output layer for performing the switching sequence. A new MAS-based framework based on a reinforcement learning method, namely the  $Q$ -learning algorithm, was proposed in [19]. In this case, historical restoration experience was used for better future restoration process.
- 3) Fully distributed approach: Compared with centralized and hierarchical distributed approaches, a fully distributed approach requires no central coordinator or distribution network model to conduct service restoration. In [20], a MAS-based framework consisting of a switch agent, a load agent, and a generator agent was proposed. The performance of this framework was quantified under three different cases including full restoration, partial restoration, and alternative path restoration. In [21], four agents, including a fault zone agent,

a zone-tie agent, a down-zone agent, and a healthy-zone agent, were defined. Each agent followed expert system rules to conduct their own restoration process autonomously. A new fully distributed algorithm was developed in [22]. It considers distributed ESS support in which a switch agent restores the load after detecting, locating, and isolating a fault while a distributed ESS agent supports the distribution system in both grid-connected and islanded modes. Two fully distributed MAS-based approaches for service restoration were presented in [23] and [24]; they considered controlled DG islanding and the uncertainty of load demand together with DGs, respectively. A distributed MAS-based communication scheme using the average consensus algorithm was developed in [25] via local communications between agents for global information discovery as inputs of the optimization-based service restoration module, which would thus become robust to a disastrous event.

A broader range of service restoration methods and future directions for electric distribution systems are summarized in [26] and [27]. More recently, truck-mounted mobile emergency resources such as mobile generators and MESSs are being increasingly used for more efficient service restoration of distribution systems owing to their mobility. The literature on service restoration with mobile emergency resources includes critical load restoration by pre-positioning and/or real-time allocation of mobile emergency generators in microgrids [28], [29], development of a co-optimization service restoration framework including the dispatch of repair crews and MESSs [30], a joint service restoration framework using DGs and MESSs with both transportation and distribution networks [31], and MESS scheduling for voltage regulation via reactive power support from MESSs [32].

Extensive research has been carried out on the DSSR problem in hierarchical and fully distributed MAS-based approaches. However, to the best of our knowledge, previous studies have neither presented a MAS-based approach integrated with MESSs nor investigated the impact of MESSs on the performance of the DSSR. The novelty of this study is that it provides a hierarchical MAS-based framework that schedules the on/off operations of switches and dispatches of DGs, SESSs, and MESSs to restore the unserved load efficiently. The main contributions of this study are summarized as follows:

- 1) Compared to existing MAS-based service restoration methods in a two-layer cyber-physical architecture, excluding the dispatch of MESSs, we present a three-layer framework that consists of cyber, physical, and transportation layers corresponding to i) the communication scheme for the MAS, ii) electric distribution system with switches and DERs including DGs, SESSs, and MESSs, and iii) transportation network for MESSs, respectively.
- 2) Considering the emergency situation that requires the dispatch of MESSs, we design a communication scheme

where MESS agents cooperate with load agent (LA), switch agent (SA), DG agent (DA), and SESS agent to restore the unserved loads effectively. We adopt Dijkstra algorithm to MESS agents for determining optimal road routing paths for the MESSs. In addition, we investigate the impact of MESSs under damaged road condition on the proposed algorithm and verify that more damaged roads can change the target node of a MESS with unserved loads with a slower service restoration time.

The simulation results confirmed, under various simulation environments, that the proposed agents can be successfully coordinated to energize as much load as possible with different number of faulty lines and SESSs/MESSs while satisfying system operation constraints for nodal voltage in terms of a number of restored loads and restoration time steps, the amount of dispatch of DGs, and the state of charge of SESSs and MESSs.

The rest of this paper is organized as follows. Section II introduces the proposed MAS-based architecture along with various types of agents, and addresses the problem formulation. Section III presents the proposed MAS-based service restoration strategy. The simulation results for the proposed service restoration approach are reported in Section IV, and the conclusions are given in Section V.

## II. SYSTEM MODEL AND PROBLEM FORMULATION

### A. TYPE OF AGENT

The proposed distributed service restoration strategy is built upon a multi-agent system where the following four types of agents play a role in the restoration process.

#### 1) LOAD AGENT (LA)

Each LA is associated with its load node. The LA has the knowledge of the load ID and the amount of load demand. This agent monitors the voltage and current at its node.

#### 2) SWITCH AGENT (SA)

The SA detects the fault location and controls the switching of two adjacent switches at every node. This agent has the knowledge of the switch ID, on/off status of the switch, and the node in which the switch is deployed. Each SA communicates with the head switch agent (HSA) at the upper level, which conducts island reconfiguration for maintaining a radial topology of the distribution system.

#### 3) DG AGENT (DA)

The DA represents the generator ID, the generation capacity, and the ramping rate of the DG. The primary goal of this agent is to perform distribution power flow analysis and calculate the amount of available power generation at each time step. There are two types of DAs: (1) black start DA (BSDA) and (2) non-black start DA (NBSDA). A BSDA controls the black start generator that is capable of providing a local power support without depending on an external power source from the grid. A non-black start generator can only restart with

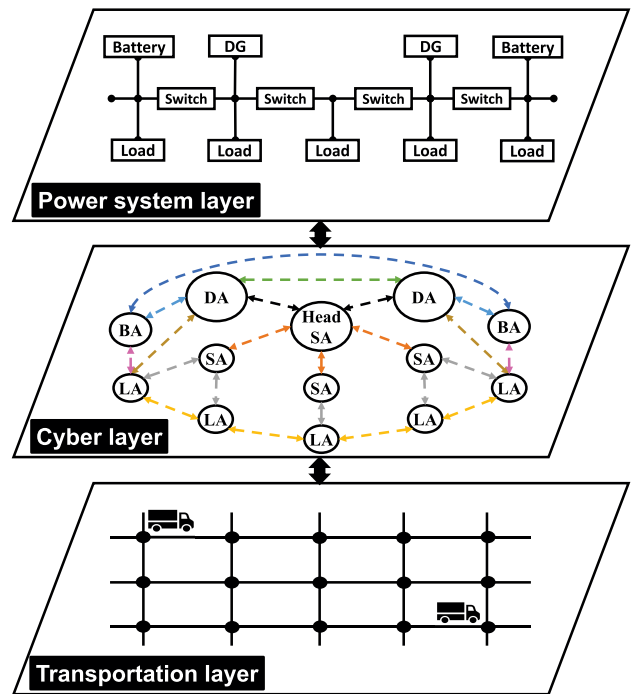


FIGURE 1. A three-layer framework illustrating the proposed MAS-based service restoration approach.

an external power support, and its operation is managed by the NBSDA.

#### 4) BATTERY AGENT (BA)

BAs are classified into two categories, namely static battery agent (SBA) and mobile battery agent (MBA), corresponding to ESS and MESS, respectively. The BA contains information one the ESS/MESS ID, location of the node to which the ESS/MESS is connected, charging and discharging power capacities, state of energy, maximum charging and discharging capabilities, the statuses of charging and discharging, and the number of MESSs in transit.

### B. ARCHITECTURE FOR MULTI-AGENT SYSTEM

A MAS provides an effective framework and mechanism for achieving a distributed and autonomous control. A MAS consists of different types of agents that are given specific roles for achieving particular tasks. In this study, we propose a MAS-based scheme where heterogeneous agents defined in the previous subsection monitor, process, and exchange service restoration-related data with each other, thereby leading to efficient and reliable service restoration.

Fig. 1 illustrates a three-layer framework that consists of a power system, and cyber and transportation layers, corresponding to: i) an electric distribution system with DGs, ESSs/MESSs, switches, and loads ii) a communication network for agents and iii) a road network for MESSs. As shown in this figure, agents interact each other in the cyber layer through information exchange to restore the unserved load in the power system layer efficiently by operating the switches

and DGs along with quick dispatch of MESSs in the transportation layer. A simple description for the communication procedure of the agents is as follows. The SA detects fault locations and informs its corresponding LA about them. Simultaneously, the SA sends the information on the fault locations to the HSA, which in turn conducts island reconfiguration based on this information to maintain a radial structure of post-fault distribution systems. Then, the LA shares the information concerning the amount of unserved load with its neighboring LAs and sends it to the corresponding DA and BA. According to the reconfigured islands with the switching status updated by the HSA, the DA communicates each other to determine the maximum generation capacity that can cover the unserved load in its own island at each time step. Similarly, through the communications among BAs (i.e., SBA and MBA), the SBA and MBA identify the capability of ESSs and MESSs for service restoration, respectively. Furthermore, the MBA calculates the optimal road routing path for a MESS and dispatches it to a destination for quick service restoration.

### C. PROBLEM FORMULATION

A general algorithm for the DSSR problem that produces the optimal operation schedule of switches and DERs is formulated as a constrained optimization problem with the following objective function and equality/inequality constraints.

#### 1) OBJECTIVE FUNCTION

The objective function for the DSSR problem is to maximize the total restored load  $P_{t,l}$  in the specified time horizon  $\mathcal{T}$  with time interval  $\Delta t$  considering load priority  $\omega_l$ .

$$\max \sum_{t \in \mathcal{T}} \sum_{l \in \mathcal{L}} \omega_l P_{t,l} \Delta t. \quad (1)$$

#### 2) CONSTRAINTS

The current in any distribution line from node  $i$  to  $j$  and the voltage at any node  $i$  at time step  $t$  should be maintained within their allowable limits, i.e.,  $I_{ij}^{\max}$  and  $V^{\min(\max)}$ , respectively,

$$I_{t,ij} \leq I_{ij}^{\max} \quad (2)$$

$$V^{\min} \leq V_{t,i} \leq V^{\max} \quad (3)$$

where  $V^{\min}$  and  $V^{\max}$  are set to 0.95 p.u and 1.05 p.u., respectively.

The total power consumption of the restored load at each time step should be less than the power provided by DGs, ESSs and MESSs.

$$\sum_{l \in \mathcal{L}} P_{t,l} \leq \sum_{g \in \mathcal{G}^{\text{DG}}} P_{t,g} + \sum_{g \in \mathcal{G}^{\text{ESS}}} (P_{t,g}^{\text{D}} - P_{t,g}^{\text{C}}) \quad (4)$$

$$+ \sum_{g \in \mathcal{G}^{\text{MESS}}} (P_{t,g}^{\text{D}} - P_{t,g}^{\text{C}}). \quad (5)$$

where  $\mathcal{G}^{\text{DG}}$ ,  $\mathcal{G}^{\text{ESS}}$ , and  $\mathcal{G}^{\text{MESS}}$  are the sets for DG, ESS, and MESS, respectively.  $P_{t,g}^{\text{C}}$  and  $P_{t,g}^{\text{D}}$  represent the charging and

discharging power of ESS ( $g \in \mathcal{G}^{\text{ESS}}$ ) and MESS ( $g \in \mathcal{G}^{\text{MESS}}$ ), respectively.

The capacity constraints of real ( $P_{t,g}$ ) and reactive power outputs ( $Q_{t,g}$ ) of any DG along with the constraint for the ramping rate ( $R_g$ ) of the real power output are expressed as:

$$b_{t,g}^{\text{DG}} P_g^{\min} \leq P_{t,g} \leq b_{t,g}^{\text{DG}} P_g^{\max}, \quad g \in \mathcal{G}^{\text{DG}}, t \in \mathcal{T} \quad (6)$$

$$b_{t,g}^{\text{DG}} Q_g^{\min} \leq Q_{t,g} \leq b_{t,g}^{\text{DG}} Q_g^{\max}, \quad g \in \mathcal{G}^{\text{DG}}, t \in \mathcal{T} \quad (7)$$

$$-R_g \Delta t \leq P_{t,g} - P_{t-1,g} \leq R_g \Delta t, \quad g \in \mathcal{G}^{\text{DG}}, t \in \mathcal{T} \quad (8)$$

where a binary decision variable  $b_{t,g}^{\text{DG}}$  determines the energization status of DG ( $b_{t,g}^{\text{DG}} = 1$ : energized,  $b_{t,g}^{\text{DG}} = 0$ : de-energized).

Equation (9) defines the operational dynamics of the state of charge (SOC) for ESS  $g \in \mathcal{G}^{\text{ESS}}$  at current time  $t \in \mathcal{T}$  in terms of the SOC at previous time  $t - 1$ , charging and discharging efficiency, i.e.,  $\eta_g^{\text{C}}$  and  $\eta_g^{\text{D}}$ , and charging and discharging power, i.e.,  $P_{t,g}^{\text{C}}$  and  $P_{t,g}^{\text{D}}$ , respectively. Equation (10) expresses the capacity constraint of the SOC for the ESS. Equations (11) and (12) present the constraint on charging ( $P_{t,g}^{\text{C}}$ ) and discharging power ( $P_{t,g}^{\text{D}}$ ) of the ESS, respectively, where  $b_{t,g}^{\text{ESS}}$  represents the binary decision variable that determines the on/off status of the ESS.

$$\text{SOC}_{t,g} = \text{SOC}_{t-1,g} + \eta_g^{\text{C}} P_{t,g}^{\text{C}} \Delta t - \frac{1}{\eta_g^{\text{D}}} P_{t,g}^{\text{D}} \Delta t \quad (9)$$

$$\text{SOC}_g^{\min} \leq \text{SOC}_{t,g} \leq \text{SOC}_g^{\max} \quad (10)$$

$$P_g^{\text{C},\min} b_{t,g}^{\text{ESS}} \leq P_{t,g}^{\text{C}} \leq P_g^{\text{C},\max} b_{t,g}^{\text{ESS}} \quad (11)$$

$$P_g^{\text{D},\min} (1 - b_{t,g}^{\text{ESS}}) \leq P_{t,g}^{\text{D}} \leq P_g^{\text{D},\max} (1 - b_{t,g}^{\text{ESS}}). \quad (12)$$

Note that the constraints (9)–(12) also hold true for MESS  $g \in \mathcal{G}^{\text{MESS}}$  along with the road routing algorithm.

Equations (13) and (14) guarantee that the real and reactive power flows from node  $i$  to  $j$  become zero if the corresponding line is not energized ( $b_{t,ij}^{\text{BR}} = 0$ ). Otherwise, they should be maintained within their allowable range when the line is energized ( $b_{t,ij}^{\text{BR}} = 1$ ).

$$b_{t,ij}^{\text{BR}} P_{ij}^{\min} \leq P_{t,ij} \leq b_{t,ij}^{\text{BR}} P_{ij}^{\max}, \quad (i,j) \in \mathcal{B}, t \in \mathcal{T} \quad (13)$$

$$b_{t,ij}^{\text{BR}} Q_{ij}^{\min} \leq Q_{t,ij} \leq b_{t,ij}^{\text{BR}} Q_{ij}^{\max}, \quad (i,j) \in \mathcal{B}, t \in \mathcal{T}. \quad (14)$$

Equation (15) limits the sudden load pickup of DGs and ESSs/MESSs at each time step to prevent a sudden drop of the system frequency [8]. In (15), the sudden incremental amount of restored loads at each step must be smaller or equal to the maximum allowable pickup power in terms of 5% ( $\xi^{\text{DG}} = 0.05$ ) and 100% ( $\xi^{\text{ESS(MESS)}} = 1$ ) of the total capacity of all energized DGs and ESSs/MESSs in discharging state, respectively.

$$\sum_{l \in \mathcal{L}} P_l (b_{t,l}^{\text{L}} - b_{t-1,l}^{\text{L}}) \leq \xi^{\text{DG}} \sum_{g \in \mathcal{G}^{\text{DG}}} b_{t,g}^{\text{DG}} P_g^{\max} + \xi^{\text{ESS(MESS)}} \sum_{g \in \mathcal{G}^{\text{ESS}} \cup \mathcal{G}^{\text{MESS}}} b_{t,g}^{\text{DG}} P_g^{\text{D},\max} \quad (15)$$

**Algorithm 1** Kruskal Algorithm-Based Island Reconfiguration

```

1 function Kruskal(edges)
2 Initialize a priority queue  $Q$  to contain all edges in  $G$ 
  using the weights as keys
3 Define a forest  $T$  empty
4 while  $T$  has fewer than  $n - 1$  edges do
5   ▷ Remove the minimum weighted edge  $(i, j)$  from  $Q$ 
6   //Prevent cycles in  $T$ . Add edge  $(i, j)$  only if  $T$  does
  not contain a path between  $i$  and  $j$  yet
7   ▷ Let  $C(j)$  be the cluster containing  $j$ , and let  $C(i)$  be
  the cluster containing  $i$ 
8   if  $C(j) = C(i)$  then
9     ▷ Add edge  $(i, j)$  to  $T$ 
10    ▷ Merge  $C(j)$  and  $C(i)$  into one cluster, that is,
    union  $C(j)$  and  $C(i)$ 
11  end
12 end
13 return tree  $T$ 

```

**Algorithm 2** Dijkstra Algorithm-Based Road Routing of MESS

```

1 function Dijkstra(network, source)
2 for each road node  $j$  in network do
3   ▷ dist[ $j$ ]:=infinity
4   ▷ previous[ $j$ ]:=undefined
5 end
6 dist[source]:=0
7  $Q$ := the set of all nodes in graph
8 while  $Q$  is not empty do
9   ▷  $i$ := node in  $Q$  with smallest dist[ ]
10  ▷ Remove  $i$  from  $Q$ 
11  for each neighbor  $j$  of  $i$  do
12    ▷ alt:=dist[ $i$ ]+dist-between( $i, j$ )
13    if alt < dist[ $j$ ] then
14      ▷ dist[ $j$ ]:=alt
15      ▷ previous[ $j$ ]:=i
16    end
17  end
18  ▷ return previous[ ]
19 end

```

where the energized load is considered only when the status of the load is switched from off at time step  $t - 1$  ( $b_{t-1,l}^L = 0$ ) to on at time step  $t$  ( $b_{t-1,l}^L = 1$ ).

**III. PROPOSED SERVICE RESTORATION STRATEGY**

**A. ISLAND RECONFIGURATION**

Given that multiple islands are created owing to multiple line faults, the network reconfiguration initiates with the operation of tie-switches. However, when some islands are merged into a single one through a closing tie-switch, the reconfigured network may not be radially structured because additional lines associated with tie-switches can make the merged island looped. To eliminate this loop, island reconfiguration is executed by the HSA.

The island reconfiguration process is carried out using a greedy Kruskal algorithm [33] based on graph theory. This algorithm is formulated as a minimum spanning tree problem that minimizes a weight inside a graph. In the graph theory literature, an undirected graph  $G = (V, E)$  is expressed in terms of  $V$ , which is the set of nodes or vertices, and  $E$ , which is the set of edges. An unordered pair  $(i, j)$  belongs to the set  $E$  if nodes  $i$  and  $j$  are connected to each other through an edge. The weight  $\omega_{ij}$  of each edge  $(i, j)$  used for island reconfiguration can be updated using (16), which represents the inverse of an absolute value of the real power flow  $P_{ij}$  at line  $(i, j)$ .

$$\omega_{ij} = \frac{1}{|P_{ij}|} = \frac{1}{\left| \Re \left( |V_i|^2 \left[ \frac{1 - V_i V_j^*}{R_{ij} - jX_{ij}} \right] \right) \right|} \quad (16)$$

where  $R_{ij}$  and  $X_{ij}$  are the values of the resistance and reactance of line  $(i, j)$ . We can observe from (16) that a higher real power flow yields a lower line loss, thus lowering the corresponding weight. As shown in Algorithm 1, the Kruskal algorithm

constructs a tree network  $T$  without loop by sequentially deleting the line with the minimum weight. The procedure followed by Algorithm 1 is summarized as follows.

An initial weight is calculated using (16). All the available edges with their corresponding weights are initialized and listed (line 2). After initializing a set  $T$  that contains the result of the algorithm (line 3), the algorithm iteratively obtains the desired radial network (line 4~12). The weighted edges are marked, spanning from node  $i$  to  $j$  (line 5). The parameter  $T$  can not be allowed to contain cycles (line 7~11). Nodes  $i$  and  $j$  are separated into its own cluster (line 7). If the edge spans from node  $i$  to  $j$ , the edge is added to  $T$  and the cluster  $C$  is updated (line 8~11). Finally, the algorithm provides the desired radial distribution network  $T$  (line 13).

**B. ROAD ROUTING FOR MOBILE ESS**

A road routing process is required for a MESS so that its optimal charging and discharging schedules can be efficiently determined. In general, the Dijkstra algorithm is used as a road routing method to find the shortest path such that the travel time of the MESS is minimized, thereby leading to more rapid restoration of the non-energized load through faster MESS dispatching.

The Dijkstra algorithm solves the problem of finding the shortest path from a source node to a destination node in a graph [34]. Given a node  $j$  inside a graph  $G$ , the algorithm calculates the fastest route between an initial source node and the target node  $j$ . In this study, the node and edge defined in the Dijkstra algorithm represents the road node and the road, respectively, and the weight corresponds to the road length between two adjacent road nodes. The pseudocode of the Dijkstra algorithm is shown in Algorithm 2.

The Dijkstra algorithm starts with two input data, namely the road network topology, including each road length, and a source road node. The initial distance between the source node and other node  $j$  is set (line 2~4). Any node  $j$  other than the source node is assumed to have infinite distance. This infinite distance guarantees that the other nodes in the next iteration can be selected according to their minimum distance. After setting the distance from the source node to itself as zero (line 6) and storing all the nodes from the graph to the set  $Q$  (line 7), the iterative algorithm proceeds until all the nodes are eliminated from the set  $Q$  in the subsequent procedure (line 8~19). The node  $i$  with the smallest distance from the source node is deleted from  $Q$  (lines 9 and 10). For each unvisited neighboring node  $j$  to node  $i$  (line 11), the temporary distance from  $i$  to  $j$ , namely  $alt$ , is calculated (line 12). If  $alt$  is less than the known distance for node  $j$ , the distance for node  $j$  is updated (line 13~16). The visited node  $j$  is updated if all the neighboring nodes of node  $i$  are already calculated (line 15). The iteration goes back to line 8 with the updated node  $i$ .

Note that some roads can be severely damaged owing to extreme weather conditions. In this situation, the damaged roads are excluded prior to the execution of the Dijkstra algorithm.

### C. GENERATION OF ENERGIZATION SEQUENCE

In the reconfigured islands resulting from Algorithm 1, a feasible energization sequence for the optimal switching operations can be calculated and generated by the DA. The generated switching sequence is then sent to the SA that controls the on/off status of the switches to energize the corresponding switchable lines. The proposed algorithm for energization sequence generation is shown in Algorithm 3. This algorithm initiates by constructing the branching table (line 1), which includes multiple paths from one source node to different destination nodes. These multiple paths can be constructed to restore the unserved multiple loads based on their load priorities. A simple numerical example to show how to construct the branching table is provided in the next section. “Time step” denotes the cumulated iteration time slot whenever the energization sequence is generated. “Load in time step” and “Load demand in time step” represent the total restored load and the sum of load demand at each time step, respectively. After setting the initial value for the aforementioned three variables (line 2~4), the algorithm proceeds provided that the total generation is larger than the total load demand (line 5~34). Here, the total generation is given by the sum of all the generation outputs from DGs and ESSs and the total load demand is defined as the sum of the load demand at the considered time step for each consecutive time step. At each time step, the restorable load is iteratively selected provided that Gen pickup is larger than the load demand at that time step (line 8). Through distribution power flow analysis, which makes use of the load demand including the load with the highest load priority, potential violations of the operation constraints of the distribution system are

### Algorithm 3 Energization of Switchable Lines

```

1 Construct the branching table
2 Time step = 1
3 Load in time step = 1
4 Load demand in time step = 0
5 while Total generation > Total load demand do
6   ▷ Gen pickup=0.05×Generation+Battery discharge
7   ▷ Search for loads with high priority in each row of
   the branching table
8   while Generation pickup > load demand in time step
   do
9     ▷ Select the load with the highest load priority
   from the branching window
10    ▷ Calculate the load demand
11    ▷ Conduct distribution power flow analysis
12    if Constraint is violated then
13      ▷ Exclude the load from the branching
   window in the branching table
14      ▷ Continue
15    else
16      ▷ Choose the load with higher priority
17      if Battery status is not set then
18        if Maximum ramping rate < Generation
   pickup then
19          ▷ Battery status=charge
20          ▷ Continue
21        else
22          ▷ Battery status=discharge
23          ▷ Continue
24        end
25      end
26      ▷ Energize the load by DG and/or ESS
27      ▷ Load demand in time step += load demand
28      ▷ Load in time step += 1
29      ▷ Battery status = not set
30    end
31  end
32  ▷ Load demand in time step = 0
33  ▷ Timestep+=1
34 end

```

tested (line 9~11). If no violation is identified, the DGs and ESSs restore the load at each iteration (line 17~29). The ESSs charge power when there is a surplus generation pickup of DGs compared to the maximum ramping rate of DGs. Otherwise, the ESSs discharge power. After restoring the load by DGs and/or ESSs, the load demand at each time step is updated and the load count at the time step increases by one (line 26~28). Finally, the amount of load demand at each time step is reset and the time step is increased by one.

### D. SUMMARY OF THE PROPOSED STRATEGY

When single or multiple faults occur in the distribution system, the agents defined in Section II-A communicate with

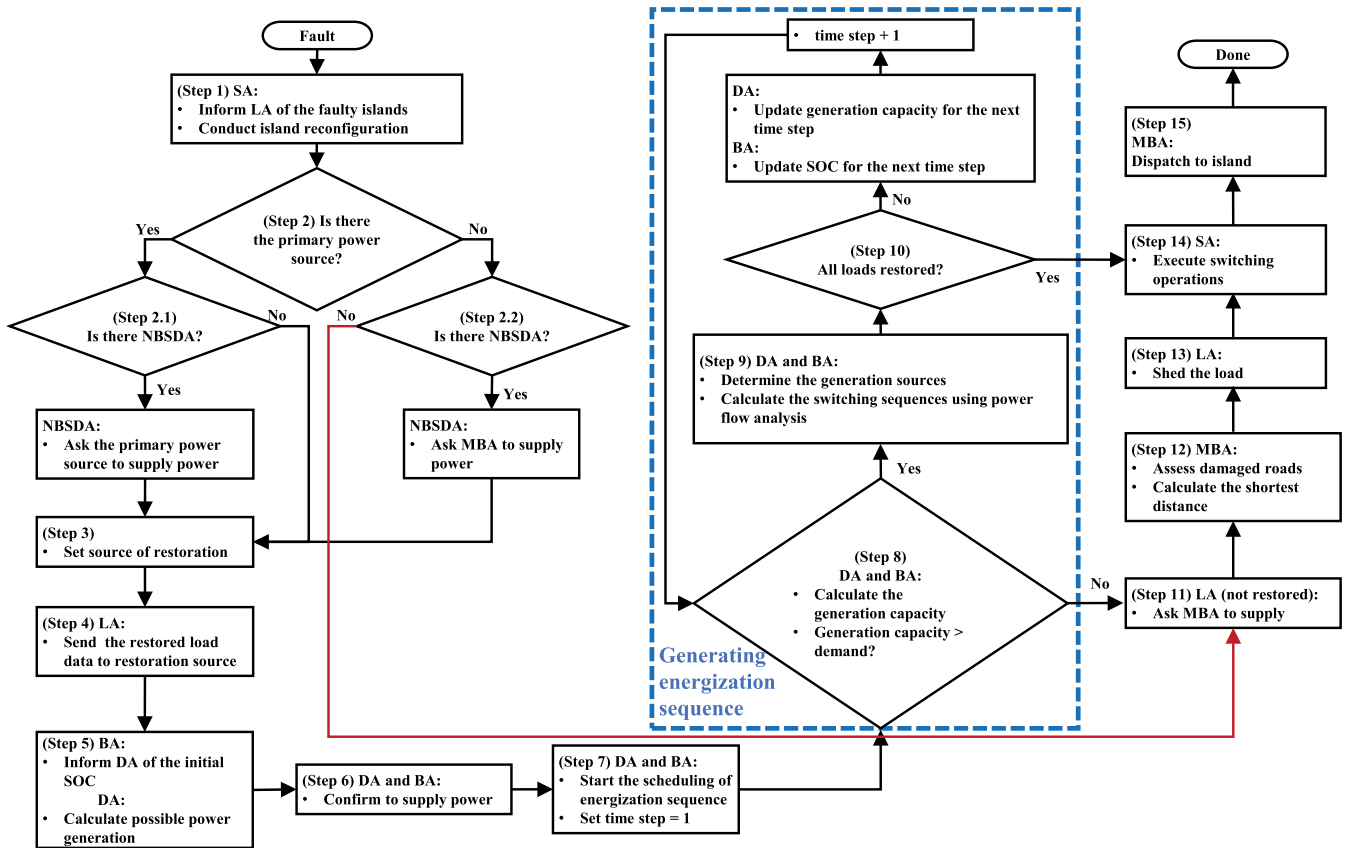


FIGURE 2. Flowchart of the procedure of the proposed service restoration.

each other to restore the load in the islands efficiently and reliably. The agents make a decision based on the island that is formed by the fault location. The decision includes the scheduling of the switching sequence and the dispatch of DGs, ESSs, and MESSs. The procedure followed by the proposed multi-agent service restoration strategy is illustrated in Fig. 2. This procedure involves the following fifteen steps:

- Step 1): Single or multiple islands are formed as a result of a faulty location. The SA informs the LA about the faulty location and performs the corresponding island reconfiguration.
- Step 2): In this step, the existence of the primary (black start distributed generator (BSDG) and ESS) and secondary (non-black start distributed generator (NBSDG)) power sources in each island is checked. Note that the secondary power source requires the power support from the primary source to start its power generation.
  - Step 2.1): If the island consists of the primary and secondary power sources, the NBSDA requests power from the primary source.
  - Step 2.2): If the island contains only the NBSDG, the NBSDA requests the MBA to supply power to the NBSDG by

dispatching MESSs. If no primary and secondary power sources are located in the island, the load restoration can be done only by MESSs, whose dispatch is performed by the MBA.

- Step 3): In each island, the power sources for load restoration and the corresponding agents (i.e., DA and BA) are identified and prepared.
- Step 4): The LA sends information on the amount of load demand to the DA and BA defined in Step 3).
- Step 5): The DA calculates the available generation capacity of the DG, and the BA informs the DA about the initial SOC of the ESSs.
- Step 6): By comparing the available power of the DGs/ESSs with the load demand, the DA and BA in the island confirm that they supply their power to the load.
- Step 7): Algorithm 3 described in Section III-C initiates with a time step=1 and proceeds through multiple iterations while the generation capacity is sufficient to support the loads in the island.
- Step 8): According to the communication with the DA and the BA, the total generation capacity is calculated by adding up the capacity of the DGs and ESSs.

- Step 9): If the total generation capacity is larger than the total load demand, the DA and BA determine the power sources for load restoration. Then, the DA conducts power flow analysis of the distribution system at each time step and determines the restored loads without violating the operation constraints of the distribution system. Finally, the DA calculates the switching sequence using the results from power flow analysis.
- Step 10): If more loads need to be restored, the DA updates the generation of the DG for the next time step according to the following equation:

$$P_{t+1,g} = P_{t,g} + R_g \Delta t. \quad (17)$$

In addition, the BA updates its SOC after energizing the loads at time step  $t$ .

$$SOC_{t+1} = SOC_t - \frac{\Delta t}{Q^{cap}} \sum_{i \in \mathcal{T}} P_{t,g}^{C(D)} \quad (18)$$

where  $Q^{cap}$  is the energy capacity (Wh) of the ESS, and  $P_{t,g}^{C(D)}$  is the charging (discharging) power at time step  $t$ . If there is no more load that can be restored, then it goes to Step 14).

- Step 11): If there is no power source or the energization sequence calculated from Step 9) is insufficient for complete load restoration, the LA requests the MBA to supply power.
- Step 12): Using Algorithm 2 introduced in Section III-B, the MBA identifies the damaged roads and, after excluding them, calculates the shortest path from the source node to the destination node with the unserved loads.
- Step 13): If the aforementioned energization procedure including MESS dispatch can not restore the load completely, load shedding is performed.
- Step 14): According to the switching sequence calculated from Step 9), the SA turns the switches on or off.
- Step 15): According to the road path calculated from Step 12), the MBA dispatches MESSs to the destination node.

Finally, Fig. 3 shows the communication scheme among agents for service restoration. The SA initiates the restoration process by sending the fault information to the LA and DA, which acknowledge it. Simultaneously, the fault information is delivered by the SA to the HSA, which performs the island reconfiguration to maintain a radial topology of the distribution system. The LAs request the amount of unserved load to the DA and BA. The DA requests the load demand and network topology after island reconfiguration to the LA and HSA, respectively. The DA then requests the power support for a black-start capability if the DA controls only the NBSDG. If the DA manages the BSDG, then it will request the power from the BA as the supplementary power for restoration. The DA then calculates the energization switching sequence based on the available data at every

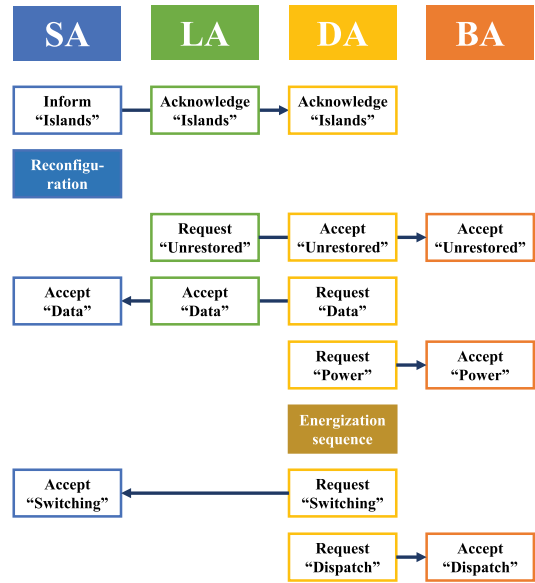


FIGURE 3. Illustration of the communication scheme among agents.

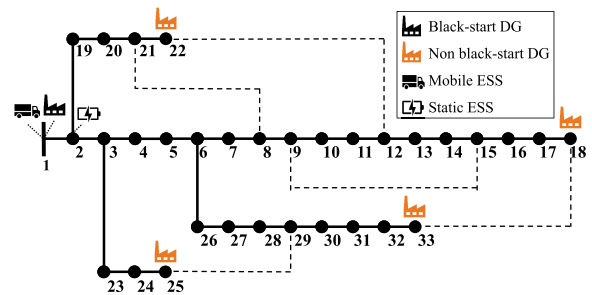


FIGURE 4. Modified IEEE 33-bus test system.

time step while satisfying all the system operation constraints. The switching sequence calculated by the DA is sent to the SAs via the HSA, which controls the status of the switches. Finally, based on the results from the previous energization process, the DA requests the MBA to dispatch its MESS.

## IV. SIMULATION RESULTS

### A. SIMULATION SETUP

In this section, we analyze the performance of the proposed MAS-based approach for service restoration in the modified IEEE 33-bus distribution test system, as shown in Fig. 4. The IEEE 33-bus system is modified with the following additional equipment: one BSDG at the substation, one SESS at node 2, four NBSDGs at nodes 18, 22, 25, and 33, and five tie-switches between pairs of nodes (8, 21), (9, 15), (12, 22), (18, 33), and (25, 29). Initially, one MESS is assumed to be connected to the substation. This MESS is in turn assumed to have an average speed of 30 km/h and require five minutes for transit time. Tables 1 and 2 show the operation characteristics of the five BSDGs/NBSDGs and three SESSs/MESSs, respectively. In Table 2, a road node is an intersection between the corresponding two road branches. In this simulation, the road nodes include all the electrical

**TABLE 1. Profiles of BSDG and NBSDG in the IEEE 33-bus system.**

DG ID	DG1	DG2	DG3	DG4	DG5
Type	BS	NBS	NBS	NBS	NBS
Bus Number	1	18	22	25	33
Road Node Number	31	14	10	43	25
Maximum Real Power (kW)	5,000	1,000	800	1,000	800
Maximum Reactive Power (kVAr)	5,000	800	600	800	800
Ramping rate (kW/min)	500	250	160	200	160

**TABLE 2. Profiles of SESS and MESS in the IEEE 33-bus system.**

Static ESS	ESS ID	ESS1	
	Bus Number	2	
	Capacity (kWh)	200	
	Maximum Real Power (kW)	200	
Mobile ESS	MESS number	MESS1	MESS2
	Bus Number	1	33
	Capacity (kWh)	300	300
	Maximum Real Power (kW)	300	300
	Road Node Number	31	25

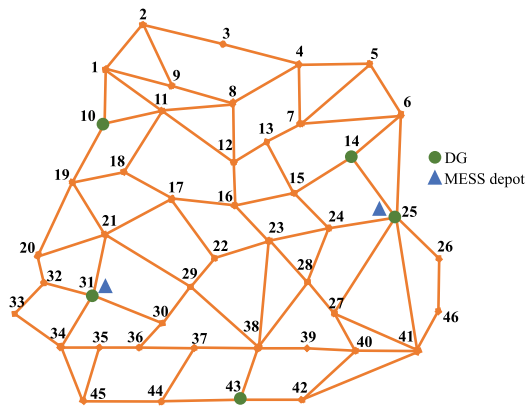


**FIGURE 5. Road topology.**

buses with additional fourteen road nodes as shown in Fig. 5 where the charging stations for MESSs are marked with green dots, corresponding to road nodes 25 and 31.

The generation capability of the NBSDGs at road nodes 10, 14, 25, and 43 corresponding to bus 22, 18, 33, and 25 can be supported by the MESSs. The weight  $\omega_l$  for the  $l$ -th load priority is randomly generated from 1 to 10 based on a uniform distribution. For simplicity, the weight is classified into three levels, from 1 to 3, where the largest number represents the highest priority. The energization sequence is generated at every time step with a one-minute time interval.

In our simulation study, three cases were tested in the IEEE 33-bus system according to the number of islands after island reconfiguration with different number of fault lines:

- Case 1: one island with three fault lines
- Case 2: two islands with one fault line
- Case 3: four islands with seven fault lines

To investigate the impact of the SESSs and MESSs on the performance of the proposed approach, each case above

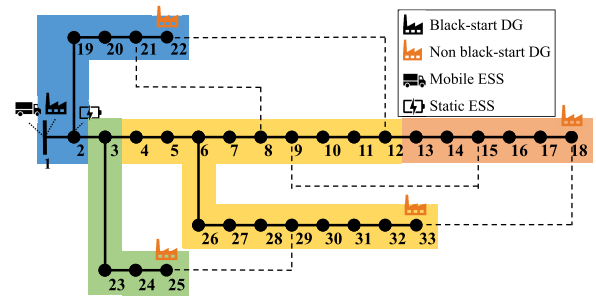


**FIGURE 6. Four islands after three fault lines in Case 1.**

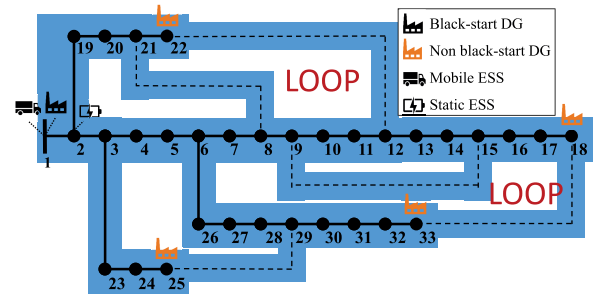


**FIGURE 7. One island with two loops before reconfiguration in Case 1.**

includes the following four scenarios with different numbers of SESSs and MESSs:

- Scenario 1 (S1): no SESS and no MESS
- Scenario 2 (S2): one SESS
- Scenario 3 (S3): one SESS and one MESS
- Scenario 4 (S4): one SESS and two MESSs

We assume that all the switches become open when the faults occur and the proposed restoration strategy initiates. The proposed service restoration approach is implemented in a computer (AMD Ryzen 7 2700X, 8 cores clocked at 3.7 GHz with 32-GB RAM in 64-bit operating system) using MATLAB R2019b along with MATPOWER 7.0 to conduct distribution power flow analysis.

**B. CASE 1**

Case 1 considers the situation in which there are three fault lines (line 2-3, line 3-4, and line 12-13). These faults give rise to four islands, as shown in Fig. 6. This fault information is delivered by the SAs to the two types of agents: i) LAs for the calculation of the amount of restorable load, and ii) the HSA for island reconfiguration. During the island reconfiguration process, the HSA conducts the following two steps: i) formation of the loops using the four tie-switches in Fig. 7, and ii) reconfiguration of the network with the loops to achieve a radial network by disconnecting the lines 6-7 and 9-10 using the Kruskal algorithm (Algorithm 1) in Fig. 8. The topology information of the radial network after island reconfiguration is then sent to the DA, which in turn generates the energization sequence.

To generate the energization sequence, the HSA first constructs the branching table. This branching table includes the load restoration paths that are constructed by energizing

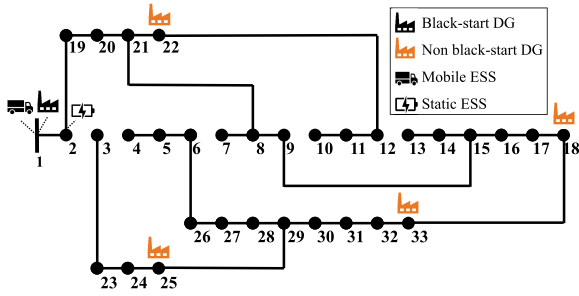


FIGURE 8. One island after reconfiguration in Case 1.

**Initial Branching Table**

Row 1	1	2	19	20	21	8	9	15	16	17	18	33	...
Row 2	1	2	19	20	21	8	9	15	16	17	18	33	...
Row 3	1	2	19	20	21	8	7	0	0	0	0	0	...
Row 4	1	2	19	20	21	22	12	11	10	0	0	0	...
Row 5	1	2	19	20	21	8	9	15	14	13	0	0	...

**Updated Branching Table**

Row 1	1	2	19	20	21	8	9	15	16	17	18	33	...
Row 2	1	2	19	20	21	8	9	15	16	17	18	33	...
Row 3	1	2	19	20	21	8	7	0	0	0	0	0	...
Row 4	1	2	19	20	21	22	12	11	10	0	0	0	...
Row 5	1	2	19	20	21	8	9	15	14	13	0	0	...

FIGURE 9. Updated branching table.

the switchable lines based on load priorities. The branching table has  $m$  rows, where  $m$  is the total number of paths from one source node (node 1) to multiple end nodes. Fig. 9 shows an example of how the branching table is updated in Case 1 with S1. In this example, the source node is node 1, and the end nodes are nodes 7, 10, 13, 3, and 4. Thus, a total of five paths ( $m = 5$ ) are considered. As shown in Fig. 8, no branch split is identified in the path from node 1 to node 21. Therefore, the elements from the second column to the sixth column in each row of the branching table are identical. However, a branch split occurs at node 21, leading to line 21-8 and line 21-22. Consequently, the seventh column (with orange color) of the branching table is updated with the end node numbers (8 and 22) of these two lines, as shown in the initial branching table in Fig. 9.

This column, highlighted with orange color, is defined as the branching window. Let us assume that the load at node 9 has a high load priority. Given that node 8 is in the same row as node 9, the load restoration for node 8 is initiated by Algorithm 3. If no constraint violation occurs in Algorithm 3, the branching window is shifted to the right with the updated window [9, 9, 7, 22, 9] as shown in the updated branching table in Fig. 9. Note that the branching window for row 4 does not shift to the right. This is because the path associated with row 4 excludes node 9. The aforementioned process for branching table updating continues

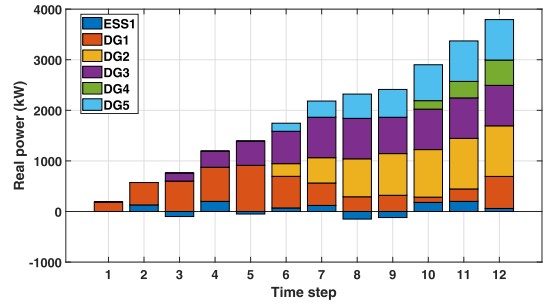


FIGURE 10. Real power of one SESS and five DGs in S2 for Case 1.

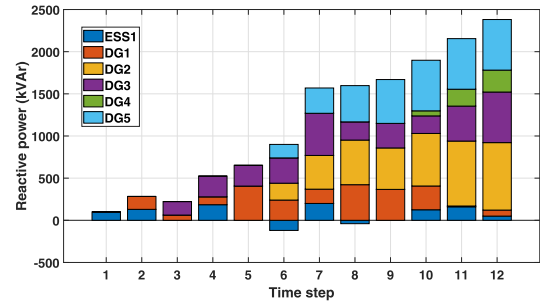


FIGURE 11. Reactive power of one SESS and five DGs in S2 for Case 1.

until the branching window reaches the end node, as long as the calculated energization sequence is feasible. Once the final energization sequence is calculated, the DA sends the result of the calculated switching sequence to the HSA, which in turn delivers it to the SAs. If the available power of the DGs is insufficient, the BA commands to discharge the power of the SESSs and MESSs. If the DGs and SESSs/MESSs do not restore the load with the energization sequence, load shedding must be finally conducted according to the result of the energization sequence.

We observe from Table 3 that the number and amount of restored loads are identical for the four scenarios in Case 1. However, note that the total number of restoration time steps in each scenario is listed in decreasing order, namely: S1 > S2 > S3 > S4. We can conclude from this observation that an increasing number of ESSs and MESSs results in a faster restoration. Table 4 compares the result of the restoration sequence between S1 and S2 in Case 1. We can see from this table that loads with a high priority such as L19, L9, and L29 are restored earlier in S2 than in S1. This is because the ESS at  $t = 1$  enables the NBSDGs to start earlier, which in turn increases the total capacity of the generation sources and the maximum load pickup associated with the frequency response rate, thereby leading to a reduction of the total restoration time steps. Note from Table 4 that no load restoration is conducted at time step 8 in S2, where the violation of the voltage constraint occurs.

Figs. 10 and 11 show the dispatch schedules of the real and reactive power from five DGs and an ESS in S2. The negative and positive powers of the ESS correspond to the charging and discharging states, respectively. Note in this figure that

TABLE 3. Summary of test cases and scenarios.

Case	Fault lines	Islands	Calculation	Scenario			
				S1	S2	S3	S4
1	2-3, 3-4, 12-13	1	Number of restored loads	33	33	33	33
			Total amount of restored loads (kW)	3,715	3,715	3,715	3,715
			Time steps	15	12	11	9
			Objective value	1,971.67	2,752.50	2,832.22	3,013.24
			Computation time (s)	0.87	0.89	1.13	1.27
2	1-2	2	Number of restored loads	-	33	33	33
			Total amount of restored loads (kW)	-	3,600	3,715	3,715
			Time steps	-	26	20	18
			Objective value	-	883.42	1,305.71	1,669.52
			Computation time (s)	-	0.95	1.18	1.26
3	2-3, 3-4, 6-7, 12-13, 15-16, 20-21, 25-29	4	Number of restored loads	4	4	33	33
			Total amount of restored loads (kW)	280	280	3,625	3,715
			Time steps	1	1	43	25
			Objective value	118.27	118.272	560.72	938.01
			Computation time (s)	0.04	0.05	1.20	1.31

TABLE 4. Restoration sequence for Case 1 (S1 and S2).

Time step	Load/DG/ESS restored	
	S1	S2
1	DG1, L1, L2, L19	DG1, ESS1, L1, L2, L19
2	L20, L21	L8, L20, L21
3	L8	DG3, L22
4	DG3, L22	L7, L9, L12, L15, L11
5	L7, L9	L10, L14, L16
6	L10, L11, L12, L15	DG2, DG5, L13, L17, L18, L33
7	L13, L14, L16	L30, L31, L32
8	DG2, DG5, L17, L18, L33	-
9	L31, L32	L29
10	L29, L30	DG4, L25, L28
11	DG4, L25	L23, L24, L27
12	L28	L3, L4, L5, L6, L26
13	L24	-
14	L3, L5, L6, L23, L26, L27	-
15	L4	-

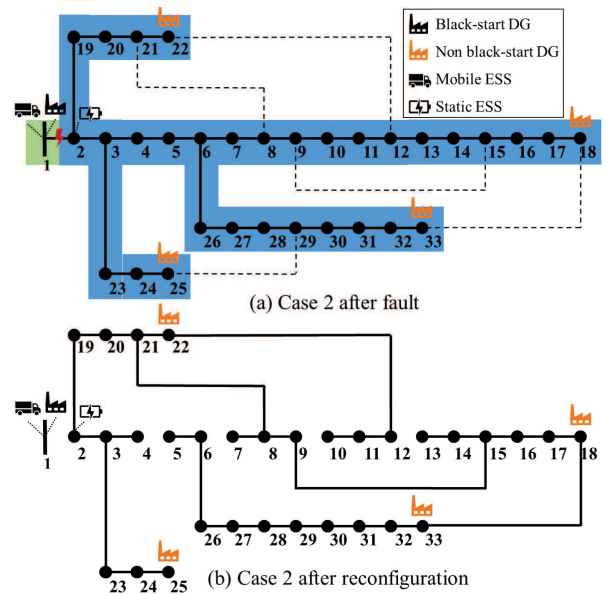


FIGURE 12. Topology of Case 2.

the dispatched real power does not violate the DG ramp rate constraint and that the ESS can support the restoration by injecting reactive power as well as by stabilizing the system by absorbing reactive power.

C. CASE 2

In Case 2, we assume that a single line fault (line 1-2) generates two islands. As shown in Fig. 12, these two islands can be maintained with a radial topology structure through island reconfiguration by disconnecting lines 4-5, 6-7, 9-10, 12-13, and 25-29. In Fig. 12, it is observed that DG1 (BSDG) is located in one island including only the substation and DG2~DG5 (NBSDGs) is located in the other island. The results of S1 in Case 2 reported in Table 3 show that the proposed approach calculates an infeasible solution for load restoration. This is expected because all the DGs in the island separated from the substation are NBSDGs without black-start capability. By contrast, it can be observed in S2~S4 that the proposed approach successfully restores the

load where the ESS and/or MESS can supply power for the NBSDGs to turn on for the load restoration. Note that the amount of restored load in S2 is less than in S3 and S4. This is because load shedding occurs at some time step where the total load demand is larger than the total generation in the island. Finally, similar to the observation from Case 1, in Case 2 it is also observed that the total number of restoration time steps decreases as the ESS and/or MESS further contribute to the load restoration.

D. CASE 3

In Case 3, the distribution system is assumed to have seven fault lines (lines 2-3, 3-4, 6-7, 12-13, 15-16, 20-21, and 25-29), which leads to seven islands. After island reconfiguration, the seven islands are merged into four, as shown in Fig. 13. We first observe from Table 3 that the total number of restored loads in both S1 and S2 are four, corresponding to L1, L2, L19, and L20 in one island. This observation

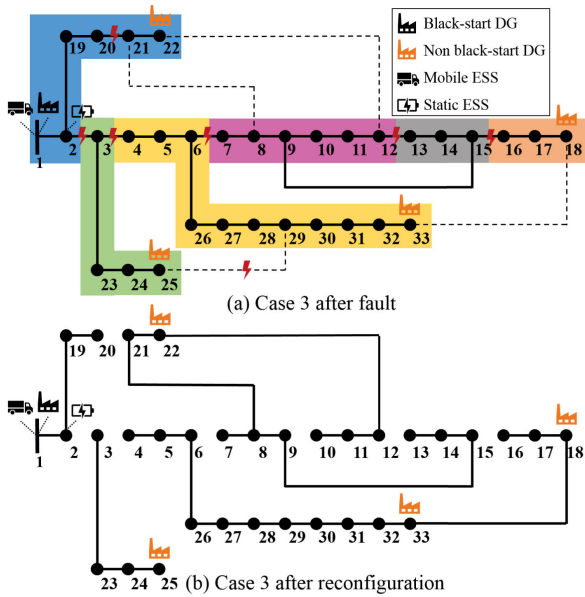


FIGURE 13. Topology of Case 3.

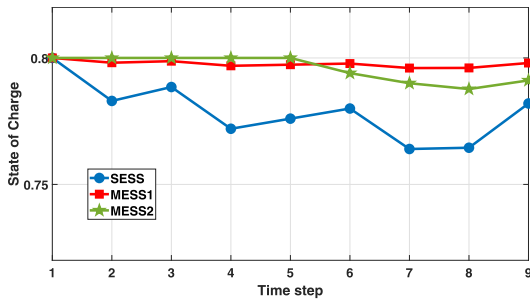


FIGURE 14. SOC of SESS, MESS1, and MESS2 in S4 for Case 1.

is because the other islands have only NBSDAs without black-start capability. Another observation is that the total number of restoration time steps in S3 is the highest one among the four scenarios. This is because only one MESS is dispatched to supply power to the loads in all the islands. By contrast, two MESSs are coordinated in S4 to restore the load in all the islands, thereby yielding shorter restoration time steps than in S3.

In addition, the total computation time for the proposed approach in all cases and scenarios is provided from Table 3. Here, the total computation time implies the sum of the execution times for: i) Algorithms 1 and 3 under S1 and S2, and ii) Algorithms 1, 2, and 3 under S3 and S4. We observe from Table 3 that the proposed approach requires a small computation time less than two seconds. This observation justifies that the proposed approach is computationally efficient and practical for real-time service restoration.

**E. SOC OF ESS AND VOLTAGE MAGNITUDE RESULTS UNDER DIFFERENT CASES AND SCENARIOS**

Figs. 14, 15, and 16 show the scheduled SOC of the SESS, MESS1, and MESS2 in S4 for Cases 1, 2, and 3,

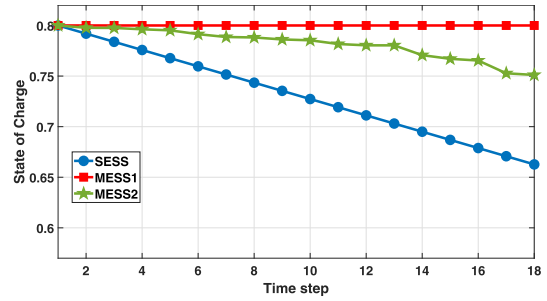


FIGURE 15. SOC of SESS, MESS1, and MESS2 in S4 for Case 2.

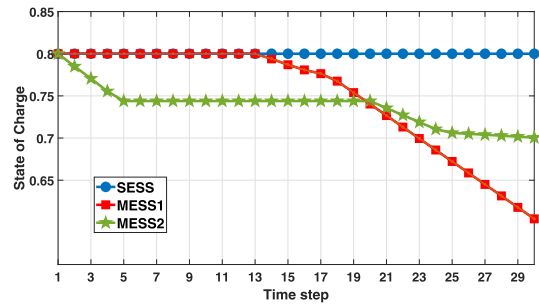


FIGURE 16. SOC of SESS, MESS1, and MESS2 in S4 for Case 3.

respectively. We observe from Fig. 14 that in Case 1 three ESSs conduct the charging or discharging processes at each time step, thus increasing or decreasing the SOC level. During the discharging process at a certain time step, all ESSs contribute to the restoration of loads. In particular, it is observed from this figure that, after some time steps, the ESS charges more power than MESS1 and MESS2. This implies that the ESS charges power from the grid after restoring the loads. This charging process can be conducted because the substation is connected to the unserved load area. We observe from Fig. 15 that in Case 2 the SOC of the SESS decreases as the restoration time step increases and the SESS continuously restores the loads. By contrast, as shown in Fig. 14, the contribution of MESS1 and MESS2 to the restoration of the load is less than that of SESS. Due to the longer time for load restoration, MESS1 is not dispatched to the unserved load area so that the SOC of MESS1 keeps unaltered. MESS2 enables through the charging process that DG5 turns on; and then, DG5 and MESS2 start to restore the island together. We observe from Fig. 16 that in Case 3 the SOC of the SESS does not change. Thus, the ESS does not contribute to load restoration. This is because the island including the ESS has a small amount of restorable loads, which can be fully restored by DG1 in the same island. We also observe from Fig. 16 that the SOC of MESS1 and MESS2 keep unchanged in the time-step periods [1, 13] and [5, 20], respectively. These periods represent the travel time of MESS1 and MESS2 from one island to another. Another observation is that the two MESSs only discharge power during the restoration time steps. This is because there is no redundant power to use for their charging in the island.

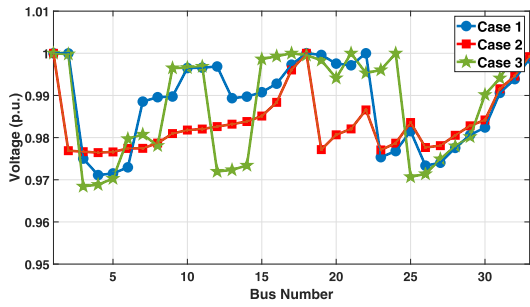


FIGURE 17. Voltage magnitudes in S3 for three cases.

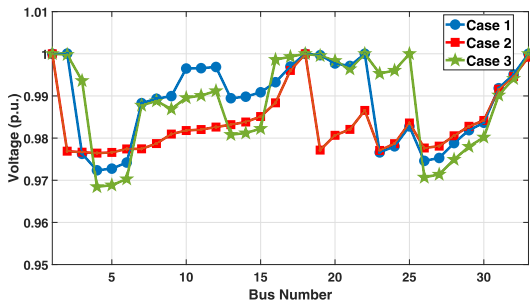


FIGURE 18. Voltage magnitudes in S4 for three cases.

Figs. 17 and 18 show the voltage magnitude results for three cases under S3 and S4, respectively. It is confirmed from these figures that the voltage magnitude at any node is maintained within its allowable limit [0.95 p.u., 1.05 p.u.]. By comparing Fig. 17 with 18, we have the following three observations. First, for Case 1, the voltage magnitude in S4 is slightly higher than in S3. This phenomenon derives from the fact that an additional MESS in S4 further increases the voltage magnitude by supplying real power to the loads. Second, for Case 2, the voltage magnitude in both S3 and S4 is identical. This is natural because MESS1 in S4 for Case 2 performs neither charging nor discharging, as shown in Fig 15, thereby leading to no impact on the voltage profile. Third, for Case 3, the voltages at buses 9, 10, and 11 are higher in S3 than in S4. This is because load shedding occurs at these three buses and the corresponding voltages increase.

**F. IMPACT OF MESS IN DAMAGED TRANSPORTATION NETWORK ON THE PROPOSED APPROACH**

In this subsection, we investigate the impact of a MESS in a damaged transportation network on the performance of the proposed service restoration method. To conduct this impact analysis in a proper way, we selected Case 3 in S4, which includes two MESSs in four islands. As shown in Fig. 19, we conducted the performance analysis of the proposed method under three different scenarios: i) scenario I: no damage, ii) scenario II: two damaged roads (19-21 and 24-28), and iii) scenario III: six damaged roads (11-18, 18-19, 19-20, 19-21, 23-24, 24-28, and 28-38). No damage scenario was selected as a base case where the depots for the MESSs are located at road nodes 25 and 31, and the target nodes

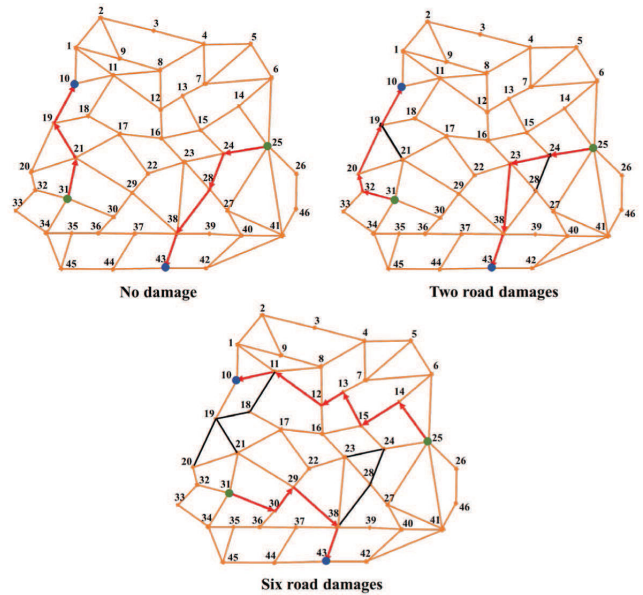


FIGURE 19. Illustration of three road topologies with no damage, two damaged roads, and six damaged roads, respectively.

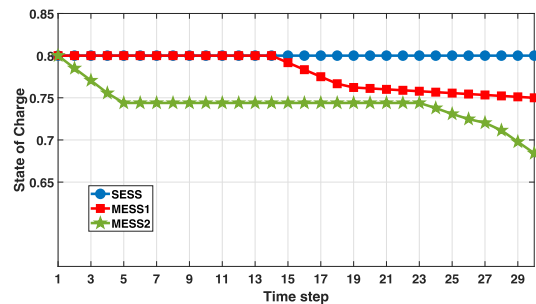


FIGURE 20. SOC of the SESS, MESS1, and MESS2 in S4 for Case 3 under road damage.

for service restoration are at road nodes 43 and 10. Table 5 compares the results of the Dijkstra algorithm among three different scenarios without and with damaged roads. We first observe from this table that as more roads are damaged, the travel distance and time for the MESSs further increase. This is because the Dijkstra algorithm selects the suboptimal routing path excluding the damaged roads. Another observation from Table 5 and Fig. 19 is that compared to scenarios 1 and 2, in scenario 3 the initial target road nodes 43 and 10 for the source road nodes 25 and 31 are changed to road nodes 10 and 43, respectively. We can conclude from this observation that, under situation of damaged road, the Dijkstra algorithm changes the target road node associated with the unserved load as well as calculates an alternative routing path for the MESS to conduct the service restoration through a quick MESS dispatch.

Fig. 20 shows the scheduled SOC of the SESS, MESS1, and MESS2 in S4 for Case 3 under scenario III. Compared to the results in Fig 16 without road damage, we observe from Fig. 20 that MESS1 and MESS2 require one and three more restoration time steps, respectively, thus leading to a

TABLE 5. Results of MESSs using the Dijkstra algorithm in Case 3 (S4) under different road conditions.

Scenario	Damaged road	From road node	To road node	Node path	Distance (km)	Travel time (minutes)
I	No damage	31	10	31-21-19-10	3.6	7.2
		25	43	25-24-28-38-43	4.45	8.9
II	19-21, 24-28	31	10	31-32-20-19-10	3.95	7.9
		25	43	25-24-23-38-43	4.9	9.8
III	11-18, 18-19, 19-20, 19-21, 23-24, 24-28, 28-38	31	43	31-30-29-38-43	4.5	9
		25	10	25-24-15-13-12-11-10	6.1	12.2

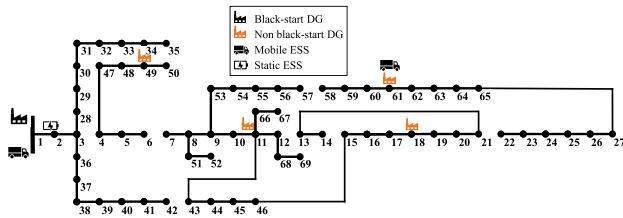


FIGURE 21. Topology of the IEEE 69-bus system after island reconfiguration.

total of 29 restoration time steps. After MESS1 supplies the unserved load in the island under a damaged road situation, the SOC of the MESS1 does not decrease significantly to maintain the rest of the loads, differing from the result shown in Fig 16. This is because the amount of unserved load without road damage is larger than with road damage. By contrast, after MESS2 restores the unserved load in a different island, the SOC of MESS2 further decreases to support the amount of unserved load that is larger than without road damage.

Finally, we evaluate the scalability of the proposed approach in the modified IEEE 69-bus distribution test system [35]. The IEEE 69-bus system is modified with the following additional equipments: one BSDG at the substation, four NBSDGs at nodes 11, 18, 49, and 61 with the generation capacities of a pair of the active and reactive power with (5 MW, 5 MVar), (0.8 MW, 0.6 MVar), (1 MW, 0.9 MVar), (1 MW, 0.9 MVar), and (2 MW, 1.8 MVar), respectively. The five tie-switches are located between pairs of nodes (11, 43), (13, 21), (15, 46), (27, 65), and (50, 59). One SESS is connected to node 2, and two MESSs are connected to nodes 1 and 61. The profiles of SESS and MESSs are the same as ones in the IEEE 33-bus system. The distribution system is assumed to have seven fault lines (lines 3-4, 6-7, 12-13, 21-22, 42-43, 50-59, and 57-58). Island reconfiguration generates four island as shown in Fig. 21. The test environment in the IEEE 69-bus system is similar to Scenario 4 under Case 3 in the IEEE 33-bus system.

The simulation result shows that the total computation time for the proposed approach is 1.34 seconds, and we verify that the proposed approach is still computationally efficient in larger distribution system. Fig. 22 shows the scheduled SOC of the SESS, MESS1, and MESS2 in the IEEE 69-bus system. We observe from this figure that the proposed approach requires a total of 26 restoration time steps to restore the unserved loads completely. In this figure, the SESS does not participate in the service restoration process because the

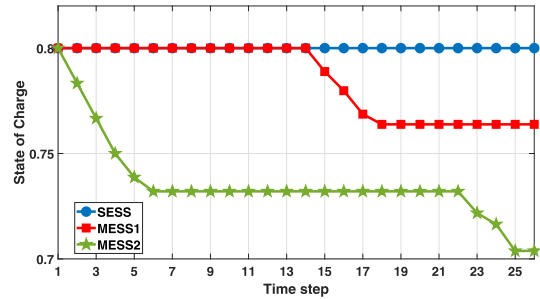


FIGURE 22. SOC of the SESS, MESS1, and MESS2 in the IEEE 69-bus system.

island including the SESS has a small amount of restorable loads, which can be completely restored by DG in the same island. Different from the result in Fig. 16, it is observed from Fig. 22 that the MESS1 and MESS2 stop discharging their power to the loads in the islands at time steps 18 and 25, respectively. This is because the capacities of DGs in the islands are large enough to supply their power to all the loads.

To the best of the authors knowledge, this work is the first MAS framework for service restoration considering the dispatch of the MESSs in active distribution systems with DGs and SESSs. The advantage and meaningful observations of the proposed approach can be summarized as follows:

- The proposed service restoration method through the coordination of heterogeneous agents for loads, switches, DGs, SESSs, and MESSs can successfully increase the total amount of restored loads and save the total number of restoration time steps while maintaining voltage quality along the distribution feeder.
- The dispatch of the MESSs significantly increases the total amount of restored loads from 280 kW (with only a single SESS) to 3,715 kW (with additional two MESSs), which is verified from Case 3 in Table 3.
- Furthermore, the total number of restoration time steps is reduced as more MESSs are dispatched to restore the unserved loads. This is verified from Case 2 in Table 3, which shows that the total number of restoration time steps under S2 (without the MESS), S3 (with a single MESS), and S4 (with two MESSs) are 26, 20, 18, respectively.
- Under situation of damaged road, the Dijkstra algorithm successfully calculates an alternative routing path for the MESS to conduct the service restoration at the expense of a slower service restoration time. This is verified from Table 5.

- The proposed approach is computationally efficient and practical for real-time service restoration. The maximum computation times in the IEEE 33-bus and 69-bus systems are 1.31 and 1.34 seconds, respectively.

## V. CONCLUSION

In this paper, we propose a hierarchical multi-agent system approach for service restoration in active distribution system with switches, distributed generators, and static/mobile energy storage systems. In the proposed approach, agents for load, switch, distributed generator, and static/mobile energy storage system communicate and cooperate with each other to restore the unserved loads due to extreme weather events and potential cyber-attacks efficiently and quickly. Various simulation results demonstrate that the proposed MAS-based approach can perform a successful service restoration under a scenario of single or multiple faults with different number of static and mobile energy storage systems while satisfying the system operation constraints.

In the future, we will extend the proposed MAS-based model to a more practical service restoration framework in a realistic unbalanced three-phase distribution system with a voltage-dependent load model. Another interesting direction for future research is to develop a robust MAS-based service restoration method considering the uncertainty of renewable distributed generators and load demands under various demand side management programs.

## REFERENCES

- [1] Z. Wang, B. Chen, J. Wang, and C. Chen, "Networked microgrids for self-healing power systems," *IEEE Trans. Smart Grid*, vol. 7, no. 1, pp. 310–319, Jan. 2016.
- [2] B. Chen, Z. Ye, C. Chen, and J. Wang, "Toward a MILP modeling framework for distribution system restoration," *IEEE Trans. Power Syst.*, vol. 34, no. 3, pp. 1749–1760, May 2019.
- [3] S. Khushalani, J. M. Solanki, and N. N. Schulz, "Optimized restoration of unbalanced distribution systems," *IEEE Trans. Power Syst.*, vol. 22, no. 2, pp. 624–630, May 2007.
- [4] Y. Wang, Y. Xu, J. He, C.-C. Liu, K. P. Schneider, M. Hong, and D. T. Ton, "Coordinating multiple sources for service restoration to enhance resilience of distribution systems," *IEEE Trans. Smart Grid*, vol. 10, no. 5, pp. 5781–5793, Sep. 2019.
- [5] R. Romero, J. F. Franco, F. B. Leao, M. J. Rider, and E. S. de Souza, "A new mathematical model for the restoration problem in balanced radial distribution systems," *IEEE Trans. Power Syst.*, vol. 31, no. 2, pp. 1259–1268, Mar. 2016.
- [6] T. Ding, Y. Lin, Z. Bie, and C. Chen, "A resilient microgrid formation strategy for load restoration considering master-slave distributed generators and topology reconfiguration," *Appl. Energy*, vol. 199, pp. 205–216, Aug. 2017.
- [7] P. L. Cavalcante, J. C. Lopez, J. F. Franco, M. J. Rider, A. V. Garcia, M. R. R. Malveira, L. L. Martins, and L. C. M. Direito, "Centralized self-healing scheme for electrical distribution systems," *IEEE Trans. Smart Grid*, vol. 7, no. 1, pp. 145–155, Jan. 2016.
- [8] B. Chen, C. Chen, J. Wang, and K. L. Butler-Purry, "Multi-time step service restoration for advanced distribution systems and microgrids," *IEEE Trans. Smart Grid*, vol. 9, no. 6, pp. 6793–6805, Nov. 2018.
- [9] B. Chen, C. Chen, J. Wang, and K. L. Butler-Purry, "Sequential service restoration for unbalanced distribution systems and microgrids," *IEEE Trans. Power Syst.*, vol. 33, no. 2, pp. 1507–1520, Mar. 2018.
- [10] Y. Xu, C.-C. Liu, Z. Wang, K. Mo, K. P. Schneider, F. K. Tuffner, and D. T. Ton, "DGs for service restoration to critical loads in a secondary network," *IEEE Trans. Smart Grid*, vol. 10, no. 1, pp. 435–447, Jan. 2019.
- [11] Y. Xu, C.-C. Liu, K. P. Schneider, F. K. Tuffner, and D. T. Ton, "Microgrids for service restoration to critical load in a resilient distribution system," *IEEE Trans. Smart Grid*, vol. 9, no. 1, pp. 426–437, Jan. 2018.
- [12] K. Chen, W. Wu, B. Zhang, and H. Sun, "Robust restoration decision-making model for distribution networks based on information gap decision theory," *IEEE Trans. Smart Grid*, vol. 6, no. 2, pp. 587–597, Mar. 2015.
- [13] X. Chen, W. Wu, and B. Zhang, "Robust restoration method for active distribution networks," *IEEE Trans. Power Syst.*, vol. 31, no. 5, pp. 4005–4015, Sep. 2016.
- [14] T. Nagata, Y. Tao, and H. Sasaki, "A multi-agent approach to power system restoration," *IEEE Trans. Power Syst.*, vol. 17, no. 2, pp. 457–462, May 2002.
- [15] A. Zidan and E. F. El-Saadany, "A cooperative multiagent framework for self-healing mechanisms in distribution systems," *IEEE Trans. Smart Grid*, vol. 3, no. 3, pp. 1525–1539, Sep. 2012.
- [16] Z. Dong, L. Lin, L. Guan, H. Chen, and Q. Liang, "A service restoration strategy for active distribution network based on multiagent system," in *Proc. IEEE Innov. Smart Grid Technol. Asia (ISGT Asia)*, Singapore, May 2018, pp. 384–389.
- [17] A. Elmitwally, M. Elsaid, M. Elgamal, and Z. Chen, "A fuzzy-multiagent service restoration scheme for distribution system with distributed generation," *IEEE Trans. Sustain. Energy*, vol. 6, no. 3, pp. 810–821, Jul. 2015.
- [18] E. Shirazi and S. Jadid, "Autonomous self-healing in smart distribution grids using agent systems," *IEEE Trans. Ind. Informat.*, vol. 15, no. 12, pp. 6291–6301, Dec. 2019.
- [19] M. J. Ghorbani, M. A. Choudhry, and A. Feliachi, "A multiagent design for power distribution systems automation," *IEEE Trans. Smart Grid*, vol. 7, no. 1, pp. 329–339, Jan. 2016.
- [20] J. M. Solanki, S. Khushalani, and N. N. Schulz, "A multi-agent solution to distribution systems restoration," *IEEE Trans. Power Syst.*, vol. 22, no. 3, pp. 1026–1034, Aug. 2007.
- [21] A. Abel Hafez, W. A. Omran, and Y. G. Hegazy, "A decentralized technique for autonomous service restoration in active radial distribution networks," *IEEE Trans. Smart Grid*, vol. 9, no. 3, pp. 1911–1919, May 2018.
- [22] C. P. Nguyen and A. J. Flueck, "Agent based restoration with distributed energy storage support in smart grids," *IEEE Trans. Smart Grid*, vol. 3, no. 2, pp. 1029–1038, Jun. 2012.
- [23] A. Sharma, D. Srinivasan, and A. Trivedi, "A decentralized multiagent system approach for service restoration using DG islanding," *IEEE Trans. Smart Grid*, vol. 6, no. 6, pp. 2784–2793, Nov. 2015.
- [24] A. Sharma, D. Srinivasan, and A. Trivedi, "A decentralized multi-agent approach for service restoration in uncertain environment," *IEEE Trans. Smart Grid*, vol. 9, no. 4, pp. 3394–3405, Jul. 2018.
- [25] C. Chen, J. Wang, F. Qiu, and D. Zhao, "Resilient distribution system by microgrids formation after natural disasters," *IEEE Trans. Smart Grid*, vol. 7, no. 2, pp. 958–966, Mar. 2016.
- [26] A. Zidan, M. Khairalla, A. M. Abdrabou, T. Khalifa, K. Shaban, A. Abdrabou, R. El Shatshat, and A. M. Gouda, "Fault detection, isolation, and service restoration in distribution systems: State-of-the-art and future trends," *IEEE Trans. Smart Grid*, vol. 8, no. 5, pp. 2170–2185, Sep. 2017.
- [27] F. Shen, Q. Wu, S. Huang, J. C. Lopez, C. Li, and B. Zhou, "Review of service restoration methods in distribution networks," in *Proc. IEEE PES Innov. Smart Grid Technol. Conf. Eur. (ISGT-Eur.)*, Sarajevo, Bosnia-Herzegovina, Oct. 2018, pp. 1–6.
- [28] S. Lei, J. Wang, C. Chen, and Y. Hou, "Mobile emergency generator pre-positioning and real-time allocation for resilient response to natural disasters," *IEEE Trans. Smart Grid*, vol. 9, no. 3, pp. 2030–2041, May 2018.
- [29] L. Che and M. Shahidehpour, "Adaptive formation of microgrids with mobile emergency resources for critical service restoration in extreme conditions," *IEEE Trans. Power Syst.*, vol. 34, no. 1, pp. 742–753, Jan. 2019.
- [30] S. Lei, C. Chen, Y. Li, and Y. Hou, "Resilient disaster recovery logistics of distribution systems: Co-optimize service restoration with repair crew and mobile power source dispatch," *IEEE Trans. Smart Grid*, vol. 10, no. 6, pp. 6187–6202, Nov. 2019.
- [31] S. Yao, P. Wang, and T. Zhao, "Transportable energy storage for more resilient distribution systems with multiple microgrids," *IEEE Trans. Smart Grid*, vol. 10, no. 3, pp. 3331–3341, May 2019.
- [32] H. H. Abdeltawab and Y. A.-R.-I. Mohamed, "Mobile energy storage scheduling and operation in active distribution systems," *IEEE Trans. Ind. Electron.*, vol. 64, no. 9, pp. 6828–6840, Sep. 2017.
- [33] D. P. Montoya and J. M. Ramirez, "A minimal spanning tree algorithm for distribution networks configuration," in *Proc. IEEE Power Energy Soc. Gen. Meeting*, San Diego, CA, USA, Jul. 2012, pp. 1–7.

- [34] A. Javaid, "Understanding Dijkstra's algorithm," *SSRN Elect. J.*, Jan. 2013, doi: [10.2139/ssrn.2340905](https://doi.org/10.2139/ssrn.2340905).
- [35] J. S. Savier and D. Das, "Impact of network reconfiguration on loss allocation of radial distribution systems," *IEEE Trans. Power Del.*, vol. 22, no. 4, pp. 2473–2480, Oct. 2007.



**PANGGAH PRABAWA** (Student Member, IEEE) received the B.E. degree in electrical engineering from the Institute of Technology Sepuluh Nopember, Surabaya, Indonesia, in 2018. He is currently pursuing the M.S. degree in electrical and electronics engineering with Chung-Ang University, Seoul, South Korea. His current research interest includes power system service restoration.



**DAE-HYUN CHOI** (Member, IEEE) received the B.S. degree in electrical engineering from Korea University, Seoul, South Korea, in 2002, and the M.Sc. and Ph.D. degrees in electrical and computer engineering from Texas A&M University, College Station, TX, USA, in 2008 and 2014, respectively. He is currently an Assistant Professor with the School of Electrical and Electronics Engineering, Chung-Ang University, Seoul. From 2002 to 2006, he was a Researcher with Korea Telecom (KT), Seoul, where he worked on designing and implementing home network systems. From 2014 to 2015, he was a Senior Researcher with LG Electronics, Seoul, where he developed home energy management systems. His research interests include power system state estimation, electricity markets, the cyber-physical security of smart grids, and the theory and applications of cyber-physical energy systems. He received the Best Paper Award from the 2012 Third IEEE International Conference on Smart Grid Communications (SmartGridComm), Tainan City, Taiwan.

...